Zoology 129 (2018) 69–81

Contents lists available at ScienceDirect

Zoology

journal homepage: www.elsevier.com/locate/zool

Skull ontogeny of extant caimans: a three-dimensional geometric morphometric approach

María V. Fernandez Blanco[a,d,*], Guillermo H. Cassini[b,c,d], Paula Bona[a,d]

[a] División Paleontología Vertebrados, Museo de La Plata, Unidades de Investigación Anexo Museo, Av. 60 y 122, 1900, La Plata, Argentina
[b] División Mastozoología, Museo Argentino de Ciencias Naturales "Bernardino Rivadavia" Av. Ángel Gallardo 470, C1405DJR, Buenos Aires, Argentina
[c] Departamento de Ciencias Básicas, Universidad Nacional de Luján, Buenos Aires, Argentina
[d] Consejo Nacional de Investigaciones Científicas y Técnicas (CONICET), Argentina

ARTICLE INFO

Keywords:
Caiman latirostris
Caiman yacare
diet and cranial shape covariation
post-hatching ontogenetic variation
tridimensional landmark estimation methods

ABSTRACT

Ontogenetic variation of cranial characters used in crocodylian phylogenetic systematics has never been studied. Furthermore, the relationship between diet and skull morphological transformation during ontogeny has not been properly explored yet. We quantify the inter- and intraspecific skull morphological variation in extant caiman species focusing on those areas relevant to systematics and, also investigate the relation between diet and morphological changes during ontogeny. We applied a three-dimensional approach of geometric morphometrics on post-hatching ontogenetic cranial series of *Caiman latirostris* and *C. yacare*. In order to incorporate incomplete material, we additionally tested four different methods of missing landmark estimation and apply the thin-plate spline interpolation. We detected morphological changes between species and during ontogeny (snout and pterygoid flanges increase their proportions and, orbits, temporal fenestrae, skull roof and foramen magnum decrease their relative size) that constitutes part of a general morphological change in the cranial ontogeny of crocodylians. Moreover, the negative allometry of the fenestrae and neurocranium and the positive allometry of the splanchnocranium in both caiman species are the plesiomorphic condition, at least, for tetrapods. Shape changes during growth were found to be related to ontogenetic changes in the diet. Dissimilarities between species seem to be related to different mechanical requirements and different use of the habitat. We found inter- and intraspecific variation in some morphological characters with systematic implications (the contact of nasals with naris, the contact of prefrontals in the midline, and the bones that border the suborbital fenestra and the proportion in which one of them participates) that are not currently considered in phylogenetic analyses.

1. Introduction

Caimaninae is a clade of neotropical alligatorid crocodylians traditionally recognized since the lower Paleocene from South America (Simpson, 1937; Bona, 2007; Pinheiro et al., 2013). Living caimanines are included within the genera *Caiman*, *Melanosuchus* and *Paleosuchus*. Taxonomically, *Caiman* and *Melanosuchus* are the most controversial genera among this group. The validity of *Caiman yacare* as a single species (or subspecies of *C. crocodilus*) and the taxonomic status of *Melanosuchus* (that implies the paraphyly of *Caiman*) are the main unresolved issues (e.g., Busack and Pandya, 2001; Hrbek et al., 2008; Oaks, 2011; Bona et al., 2017; Foth et al., 2017). The genus *Caiman* was diagnosed by Spix in 1825 by a few morphological characters related to rostrum, mandible and hind limb shapes and the number of inferior teeth inserted into the upper jaw in occlusion. Only some width and length proportions of the rostrum were mentioned concerning osteology. This short and inaccurate description does not allow discriminating *Caiman* (and also *Melanosuchus*) from other alligatorids on the basis of osteological features. This also applies to living species of caimans whose original descriptions are osteologically uninformative (e.g., Linnaeus, 1758; Daudin, 1802). As a result of this taxonomy, extant species are easily distinguishable by external morphological features such as body coloration, squamation and snout shape, but their osteology and range of variation are practically unknown. In this regard, ontogenetic variation of some cranial osteological characters used in caimanine phylogenetic systematics (e.g., midline contact of prefrontals, nasals reaching the naris) has never been studied. Consequently, exploring the evolutionary history of Caimaninae becomes a problem when assigning a fossil specimen to some species of this clade based on cranial features. Furthermore, phylogenetic hypotheses of Crocodylia sensu Benton and Clark (1988) are mostly based on extinct taxa (e.g., Brochu, 1999, 2011; Bona, 2007; Fortier et al., 2014; Salas-

* Corresponding autor at: División Paleontología Vertebrados, Museo de La Plata, Unidades de Investigación Anexo Museo, Av. 60 y 122, 1900, La Plata, Argentina.
E-mail address: victoriafernandezblanco@yahoo.com.ar (M.V. Fernandez Blanco).

https://doi.org/10.1016/j.zool.2018.06.003
Received 1 November 2017; Received in revised form 15 June 2018; Accepted 18 June 2018
Available online 21 June 2018
0944-2006/

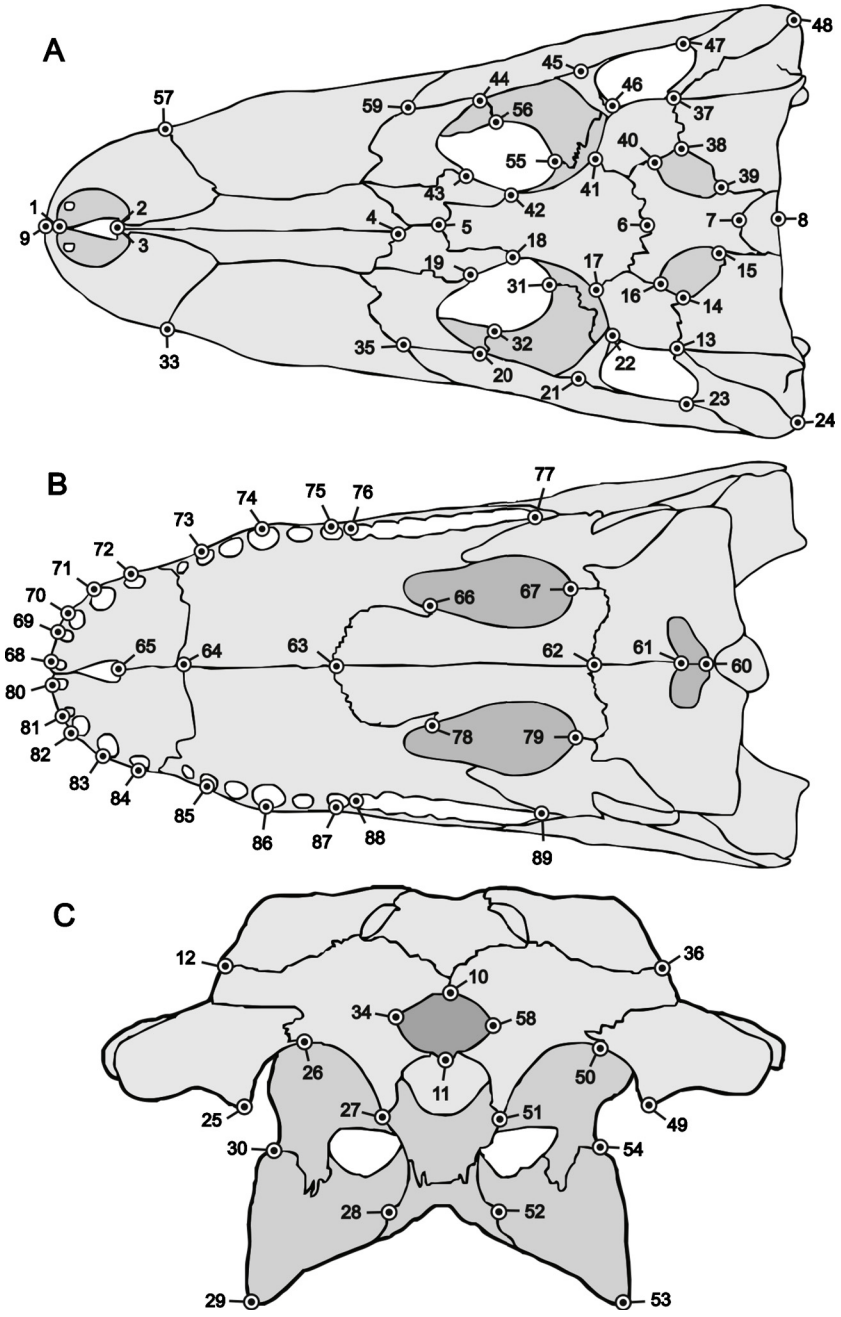

Fig. 1. Distribution of landmarks. (A). Dorsal view. (B). Ventral view. (C). Occipital view.

Gismondi et al., 2015, 2016; Hastings et al., 2016), which are known and diagnosed on the basis of skeletons, principally skulls and mandibles. Since organisms are dynamic entities and their shape is a result of processes that change throughout their life, the understanding of the osteology of living species and its ontogenetic variation is critical (Fernandez Blanco et al., 2014, 2015; Foth et al., 2015, 2017). Detecting these changes, discretizing morphological characters and analyzing them in a phylogenetic context is elemental for crocodylian systematics.

Although some analyses of ontogeny have been performed in alligatorids (e.g., Monteiro and Soares, 1997; Monteiro et al., 1997; Fernandez Blanco et al., 2014, 2015; Foth et al., 2015, 2017), the study of ontogenetic cranial trajectories in closely-related alligatorid species is a huge field to explore and essential to assess common patterns of cranial growth within a more inclusive phylogenetic context (Foth et al., 2017). Furthermore, morphological modifications in the vertebrate skull during growth could be linked to transition in diets and feeding behavior from the juvenile to the adult. It is a known fact that crocodylians eat similar food items during their life. Young specimens eat mainly invertebrates (e.g., spiders, insects, snails, crustaceans), and as they grow, crocodylians consume mostly vertebrates (e.g., fishes, amphibians, reptiles, birds and mammals) (Carvalho, 1951; Vanzolini and Gomes, 1979; Webb et al., 1982; Ayarzagüeña, 1983; Magnusson et al., 1987; Monteiro and Soares, 1997; Melo, 2002; Borteiro et al., 2008). Nevertheless, the relationship between feeding behavior and skull morphological transformation during ontogeny has not been properly explored yet.

The main goal of this study is to describe and quantify the inter- and intraspecific skull morphological variation in caimans, analyzing those areas potentially relevant to systematics and, the correlation between diet and morphological changes during ontogeny. For that purpose, we conducted a three-dimensional approach of geometric morphometrics

on post-hatching ontogenetic series of two caiman species, *Caiman latirostris* and *C. yacare*. In addition, we tested four different methods of missing landmark estimation to incorporate incomplete material and increase our data base.

2. Materials and methods

2.1. Specimens

We studied the crania of two caiman species, *Caiman latirostris* and *C. yacare*. A total of 96 specimens (73 of *C. yacare* and 23 of *C. latirostris*) were used in this study. Sample size reflects specimen availability in the visited collections even though they are the largest in the country. We sampled post-hatching growth series of both species in order to include all potential morphological changes during ontogeny. Materials are housed in the Museo de La Plata (MLP) and Museo Argentino de Ciencias Naturales "Bernardino Rivadavia" (MACN). Sex could not be determined because historical notes do not exist and an anatomical classification was not possible, either.

The specimens were assigned to three different age categories based on their size which were defined by the snout-vent length (SVL), following Santos et al. (1996) and Borteiro et al. (2008). Each animal with a SVL lower than 50 cm was considered as a juvenile, those with a SVL between 50 and 70 cm were considered sub-adults, and specimens larger than 70 cm, as adults. In our sample, skulls do not have associated body measurements. In order to assign the specimens to an age stage following the same criteria, we estimated the SVL using regression equations based on dorsal cranial length (DCL). The SVL of *C. latirostris* was estimated using the fourth equation from Table 2 of Verdade (2000). This equation was not appropriated for *C. yacare* because *C. latirostris* has a shorter snout. An equivalent equation was not available for *C. yacare* in the literature. Instead, we choose the fourth equation from Table 2 of Wu et al. (2006) for *Alligator sinensis*, assuming that *C. yacare* has a similar DCL/SVL ratio.

The *Caiman latirostirs* sample consisted of four juveniles (the smallest specimen, MLP R5801, has an estimated SVL of 47.39 cm), 10 sub-adults and 9 adults. The largest specimen of *C. latirostris* is an adult with an estimated SVL of 125.6 cm (MACN-He 1420-7375). The *C. yacare* sample consisted of seven juveniles (the smallest specimen, MLP R5053, has an estimated SVL of 43.2 cm); 32 sub-adults and 35 adults. The largest specimen of *C. yacare* (MACN-He 30637) is an adult with an estimated SVL of ~160 cm. Skulls belong to wild animals and most of them are from two provinces of Argentina (Chaco and Corrientes), six are from Paraguay, one is from Jujuy and three are undetermined (supplementary Table S1).

2.2. Landmark data

Landmarks were digitized by one of the authors (MVFB) using a Microscribe G2L digitizer (Immersion Corporation, San José, CA, USA), and were chosen in order to reflect the complete morphology of the skull. Both sides and midline points (72 and 17, respectively) were included and comprised a total of 89 landmarks (Fig. 1). Landmarks included a combination of landmarks Type I (intersection of sutures) and Type II (maximum curvature) in both views (Table 1). Previous to digitization sessions, one juvenile and one adult specimen of each species were digitized in five successive sessions to examine the consequences of the measurement error.

This study required the capture of landmarks in two blocks separately, dorsal and ventral view, in each specimen. The unification of these two landmark configurations was performed in R 3.4.1 software (R Development Core Team, 2017) with the R-function unifyVD.r written by Annat Haber, University of Chicago (available online at http://life.bio.sunysb.edu/morph/; see also Online Resource 2 from Cassini and Vizcaíno, 2012). This script binds both configurations of landmarks by means of Procrustes superposition, using the common landmarks between both views to obtain a new landmark configuration with the whole form (skull).

2.3. Missing landmark estimation

Some specimens were broken (in different degrees and sides) so, in order to maximize the number of specimens in the sample, we estimated missing landmarks. For a detailed procedure see supporting information Data S1 in the supplementary online Appendix. There are 40/73 specimens of *C. yacare* with missing landmarks, and one of them was removed from the sample because it had 32 missing landmarks. On the other hand, 15/23 specimens of *C. latirostris* have missing landmarks. Distributions of missing landmarks are reported on Supporting information Data S1 in the supplementary online Appendix. The regions of the skull more frequently broken include rostrum, skull roof, posterior palate and occipital plate (see Fig. S1 in supporting information Data S1 in the supplementary online Appendix). Those missing landmarks that could be estimated by reflection of bilateral symmetry were performed using the AMP.R script written by Annat Haber, University of Chicago (available online at http://life.bio.sunysb.edu/morph/). For the remaining missing landmarks, we have used four different methods following Arbour and Brown (2014). They included: bayesian PCA (BPCA); least-squares regression (REG); thin-plate spline interpolation (TPS); and mean substitution (MS). Subsequently, we evaluated which methods worked best with our data set. The TPS method best fitted our sample (see Results and Supporting information Data S1 in the supplementary online Appendix) and was then applied to estimate missing landmarks in incomplete specimens. The complete landmark configuration data set was exported to the software MorphoJ 1.06b to perform the geometric morphometric analysis.

2.4. Dietary information

Feeding ecology across different age categories in both species of caiman was obtained from the limited published literature. We focused on two quantitative studies with a similar approach for both species: Borteiro et al. (2008) for *C. latirostris* and Santos et al. (1996) for *C. yacare*. We selected for each age category the frequency of occurrence of prey items in stomach contents that can be found in Borteiro et al. (2008) and Santos et al. (1996). This last study provides more detail about prey groups and habitats so, in order to make the categories comparable and match those used by Borteiro et al. (2008), we aggregated these zoological classes into five categories: insects, snails, crustaceans, spiders and vertebrates. Subsequently, the reported relative frequencies were normalized following Olsen (2017) so the frequencies would sum to 1. Different habitat values described in Santos et al. (1996) were averaged (supplementary Table S2). Lastly, the five continuous dietary characters per age and species were logit transformed prior to the analysis, because the use of proportions violates assumption models (Warton and Hui, 2011). To do that, we used the function logit from the R package car 2.1-6 (Fox and Weiberg, 2011) with an adjustment factor of 0.005 to avoid proportions of zero or one.

2.5. Ontogenetic analysis

Landmark configurations were superimposed using full Procrustes fit (Dryden and Mardia, 1998) in order to remove spatial information that does not correspond to shape. This procedure minimizes the sum of squared distances between homologous landmarks by translating, rotating and scaling them to a unit centroid size (Goodall, 1991; Rohlf, 1999). A principal component analysis was performed in order to explore the main shape variations. We retained the axes (principal components) that accounted for the taxonomic and ontogenetic variation we were trying to quantify.

We assessed the extent and significance of the association between each PC and log-transformed centroid size, via a permutation test with

Table 1
Description of landmarks in dorsal and ventral views.

View	Number	Landmark definition
Dorsal	1	Contact of both premaxillae at the anterior border of the naris
	2	Contact of both premaxillae at the posterior border of the naris
	3	Anterior contact of both nasals
	4	Posterior contact of both nasals
	5	Anterior point of the frontal
	6	Contact between frontal and parietal along the sagittal plane
	7	Contact between parietal and supraoccipital along the sagittal plane
	8	Midpoint of the posterior margin of the skull roof (supraoccipital) along the sagittal plane
	9	Point at the anterior and ventral contact of both premaxillae
	10	Dorsal and middle point of the foramen magnum
	11	Ventral and middle point of the foramen magnum
	12 and 36	Lateral contact between squamosal and exoccipital
	13 and 37	Lateral contact between squamosal and postorbital above the skull roof
	14 and 38	Contact between squamosal and postorbital in the supratemporal fenestra
	15 and 39	Contact between squamosal and parietal in the supratemporal fenestra
	16 and 40	Contact between parietal and postorbital in the supratemporal fenestra
	17 and 41	Contact between postorbital and frontal on the edge of the orbit
	18 and 42	Contact between frontal and prefrontal on the edge of the orbit
	19 and 43	Contact between prefrontal and lacrimal on the edge of the orbit
	20 and 44	Contact between lacrimal and jugal on the edge of the orbit
	21 and 45	Posterior and ventral point of the orbit
	22 and 46	Point in the orbital foramen
	23 and 47	Posterior and ventral point of the infratemporal fenestra in the contact between jugal and quadratojugal
	24 and 48	Posterior contact between quadrate and quadratojugal
	25 and 49	Medial point of the articular process of the quadrate
	26 and 50	Contact between quadrate and exoccipital in the edge of the subtemporal fossa
	27 and 51	Contact between exoccipital and basioccipital in the edge of the subtemporal fossa
	28 and 52	Medial and posterior point of the pterygoid
	29 and 53	Lateral and posterior point of the pterygoid
	30 and 54	Lateral contact between pterygoid and ectopterygoid
	31 and 55	Medial and posterior point of the ectopterygoid where it contacts with the suborbital fenestra
	32 and 56	Contact between ectopterygoid and maxilla in the suborbital fenestra
	33 and 57	Lateral and ventral contact between premaxilla and maxilla
	34 and 58	Lateral point of the foramen magnum
	35 and 59	Contact between jugal, lacrimal and maxilla
Ventral	60	Posterior and middle point of the choana
	61	Anterior and middle point of the choana
	62	Contact between palatine and pterygoid along the sagittal plane
	63	Contact between palatine and maxillae along the sagittal plane
	64	Contact between maxillae and premaxillae along the sagittal plane
	65	Posterior point of the incisive foramen along the sagittal plane
	66 and 78	Contact between maxilla and palatine in the suborbital fenestra
	67 and 79	Posterior and medial point of the palatine where it contacts with the suborbital fenestra
	68 and 80	Middle point in the external surface of the alveolus of the first premaxillary tooth
	69 and 81	Middle point in the external surface of the alveolus of the second premaxillary tooth
	70 and 82	Middle point in the external surface of the alveolus of the third premaxillary tooth
	71 and 83	Middle point in the external surface of the alveolus of the fourth premaxillary tooth
	72 and 84	Middle point in the external surface of the alveolus of the fifth premaxillary tooth
	73 and 85	Middle point in the external surface of the alveolus of the second maxillary tooth
	74 and 86	Middle point in the external surface of the alveolus of the fourth maxillary tooth
	75 and 87	Middle point in the external surface of the alveolus of the sixth maxillary tooth
	76 and 88	Anterior point of the alveolar groove
	77 and 89	Posterior point of the alveolar groove

10,000 replicates in MorphoJ, in order to detect which PCs are ontogenetically informative. We performed a multivariate regression on the Procrustes coordinates against the log-transformed centroid size for each species separately, to explore how the allometric variation in shape is associated with size. The regression significance was tested by a permutation test with 10,000 replicates (Bookstein, 1991; Mitteroecker et al., 2004).

To explore the patterns of covariation between cranial morphology and diet through ontogeny of both species, we used the two-block Partial Least Squares analysis (PLS) (Mitteroecker and Bookstein, 2008). We defined the Block-1 as the cranial shape (i.e., landmark configurations) and the Block-2 as the continuous diet characters (i.e., the logit transformed diet proportions matrix). The PLS has been used to find correlated pairs of linear combinations between the two blocks accounting for the major covariation (Rohlf and Corti, 2000; Klingenberg, 2013).

All these morphometric analyses (PCA, PLS and Regressions) produce vectors in shape space (Cassini et al., 2017). We performed an angular comparison of these vector directions in order to compare the components of shared shape variations. These angles were computed as the arccosines of the signed inner products between the regression vectors (Drake and Klingenberg, 2008; Klingenberg and Marugán-Lobón, 2013, Segura et al., 2013, 2017). The angular comparison analyses include: ontogenetic trajectories (i.e., regression) of each species; the PLS analyses; a multivariate, pooled within-group regression of shape against log-transformed centroid size including both taxa; and PCA shape change vectors.

All the morphometric analyses were performed in MorphoJ 1.06b software (Klingenberg, 2011). The visualization and graphics were made using the Morpho R package 2.5.1 (Schlager, 2017) following Muñoz et al. (2017), which allows the colour pattern to be associated with shape changes.

3. Results

3.1. Missing landmark estimation

The TPS method has the smallest error and shows a slight increase when the number of missing landmarks increases (see Fig. S2 in supporting information Data S1 in the supplementary online Appendix). In the four methods, the cranial region with the biggest absolute error is located in the posterior region of the palate and in the articular condyles. The TPS method has the lowest and uniformly distributed percentage error (see Fig. S3 in supporting information Data S1 in the supplementary online Appendix).

3.2. Ontogenetic analysis

The principal components analysis (PCA) resulted in the first six PCs accounting for the 76.201% of cumulative variance. Only PC1 and PC2 showed clear taxonomic and/or ontogenetic patterns (see below). As no PC beyond PC2 was informative, only the first two principal components are described and used in the following interpretations. Only PC2 correlates significantly and positively with log-transformed centroid size ($R^2 = 0.9437$, p-value < 0.0001) and has a vector angle of 3.891° with the pooled within-group (species) regression of shape coordinates against log-transformed centroid size (p-value < 0.00001). The first component (PC1) explains the 43.65% of total variance, the second one (PC2) explains the 19.22% and altogether account for over 60% of cumulative variance. Species are separated along the PC1 with *C. yacare* situated on the negative values up to 0.01 and *C. latirostris* is from 0.04 to more positive values, with a gap between them (Fig. 2). Shape changes associated with negative values of this component show a long, narrow and low skull (Fig. 3A). In the rostrum, the premaxillae are displaced anteriorly forming a long and narrow snout; nasals are separated from the posterior border of the naris. In the orbital region, orbits open more laterally and prefrontals prevent the contact between the frontal and nasals. In the suborbital fenestrae, the pterygoid is either slightly interposed or absent between ectopterygoid and palatine. In the temporal region, the skull roof is flat and narrow with long and narrow supratemporal fenestrae and a small exposure of supraoccipital. The pterygoid flanges are short and narrow. Instead, positive values show a short, broad and high skull (Fig. 3B). Rostrally, the snout is high, short and broad. Nasals extend into the naris forming their posterior border. In the orbital region, orbits open more dorsally and frontal and nasals are in contact. At the palate, the posterior border of the suborbital fenestrae always have a broad participation of pterygoid. In the temporal region, the skull roof is flat but broad with subcircular supratemporal fenestrae and a more exposed supraoccipital. The jugal is laterally expanded, high and flexed respect to the rostrum. The pterygoid flanges are large, broad and anterolaterally displaced.

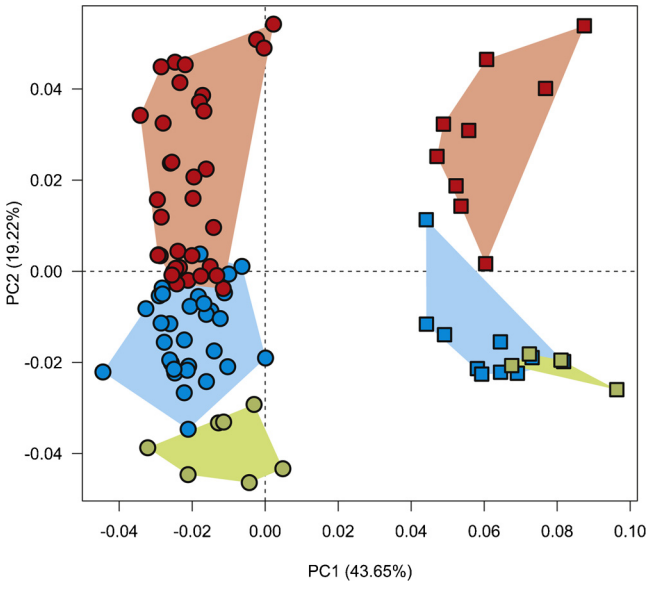

Fig. 2. Principal Component Analysis. Biplot of PC1 *vs* PC2. *Caiman yacare* (circles) and *C. latirostris* (squares). Juveniles (green), sub-adults (blue), adults (red).

The variation along PC2 comprises transformations that clustered juvenile specimens of both species towards negative values and adult specimens toward positive values. Fig. 3C shows the shape changes associated with negative values of this component (i.e., young specimens). These are characterized by low naris, short and narrow premaxilla, broad maxilla and a depressed palate forming a flat and a gracile rostrum. The palate shows long suborbital fenestrae, an anteriorly displaced choana, short and laterally displaced pterygoid flanges and a short distance between the exoccipital-basioccipital contact and the medioposterior point of pterygoid flanges. The orbital region is anteriorly displaced with large orbits that open more laterally. The temporal region comprises a high and broad skull roof, large infratemporal and supratemporal fenestrae, a laterally compressed quadrate and quadratojugal forming a short condyle, and a high occipital plate with a large foramen magnum. Toward positive values (i.e., adult specimens), the associated shape changes (Fig. 3D) include high naris, long and broad premaxilla, narrow maxilla and a ventrally displaced palate conforming a high and a robust rostrum. The palate shows short suborbital fenestrae, a posteriorly displaced choana, long and medially displaced pterygoid flanges and a large distance between the exoccipital-basioccipital contact and the medioposterior point of pterygoid flanges. The orbital region is posteriorly displaced with small orbits that open more dorsally. The temporal region is shortened and includes a narrow skull roof with a concave posterior border, a small infratemporal and supratemporal fenestrae, a lateral expanded quadrate and quadratojugal forming a long condyle, and a low occipital plate with a small foramen magnum. The PC3 (5.82%), PC4 (2.99%), PC5 (2.49%) and PC6 (2.04%) do not show a clear association with morphological changes or with ontogeny (all $R^2 < 0.001$ and p-values > 0.7217), so they will not be described.

The PLS analysis on both species (Figs. 4 and 5) show a significant relationship between shape and diet (Table 2). The PLS analysis on *C. latirostris* shows that the first pairs of PLS explains about 100% of covariation (Table 2). The PLS1 vector of block-1 was visualized as surface plus thin plate spline gridline deformations in Fig. 4B and C. The shape changes associated to the first block have a significant but high angle only with PC2 (69.107°; $p < 0.0001$) and range from a slender cranium with low naris, short and narrow premaxilla, broad maxilla and a depressed palate forming a flat and a gracile rostrum (on the negative end) to a more robust cranium with high naris, long and broad premaxilla, narrow maxilla and a ventrally displaced palate conforming a high and a robust rostrum (on the positive end). The block-2 PLS coefficients (Fig. 4A) of the five diet categories were summarized on supplementary Table S2. The spiders and crustaceans items show high negative values (ca −0.76 and −0.44 respectively) and the vertebrates item a high positive value (~0.43). The PLS1 scores show a high and significant correlation between blocks (Fig. 4A and Table 2; r = 0.896, p = 0.0001 after 10,000 rounds of permutation tests). While the juveniles lie on the double negative quadrant, the subadults lie near the zero values and the adults lie on the double positive quadrant.

The PLS analysis on *C. yacare* shows that the first pairs of PLS explains about 93% of covariation (Table 2). The PLS1 vector of block-1 was visualized as surface plus thin plate spline gridline deformations in Fig. 5B and C. The shape changes associated to the first block have a significant but acute angle only with PC2 (17.75°; $p < 0.00001$) and range from a long and narrow cranium with anteriorly displaced orbits that open more laterally, short pterygoid flanges and a quadrangular

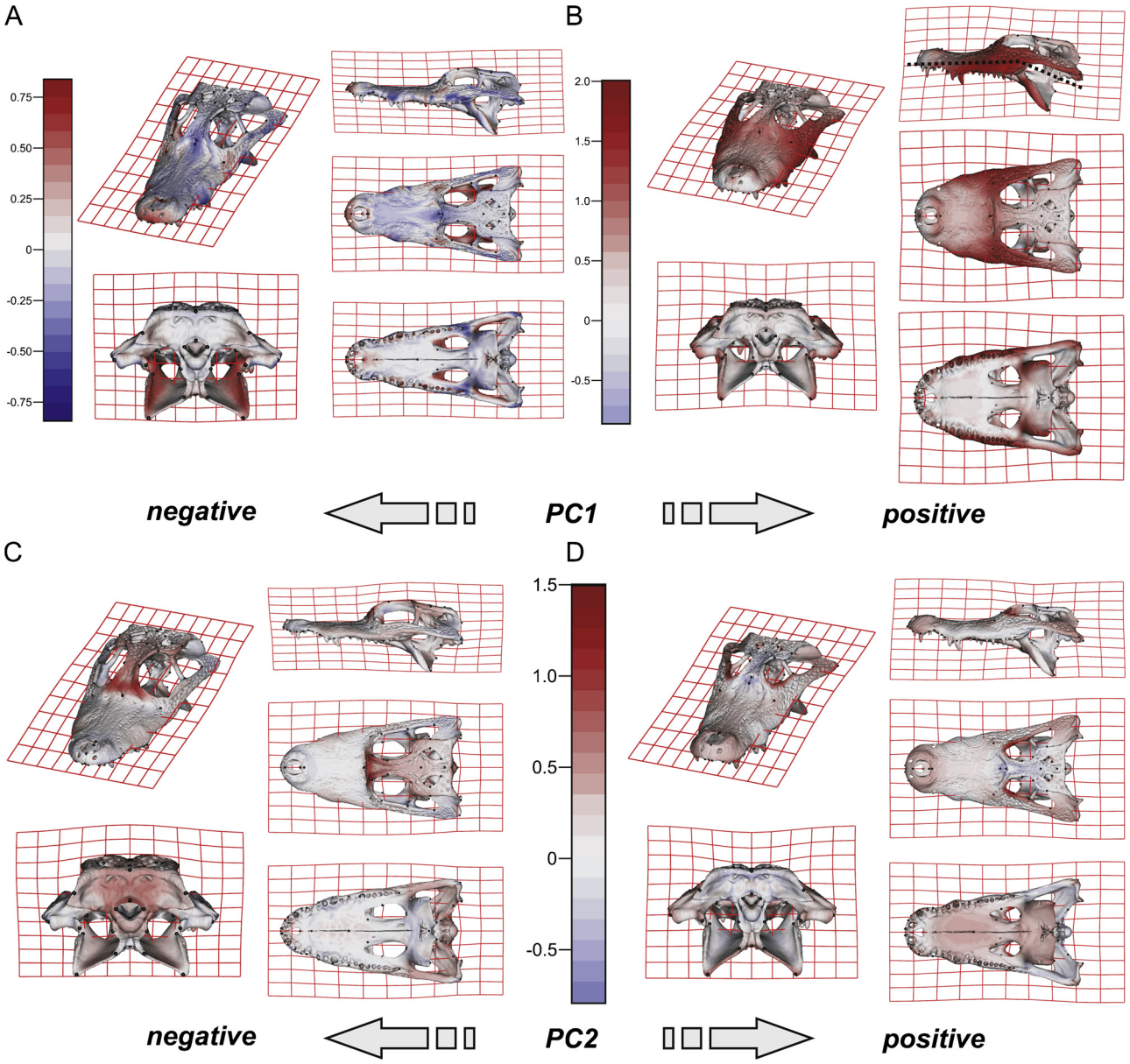

Fig. 3. Thin plate spline gridlines, coloured meshes and shape changes associated with the PC1 and PC2. (A). Thin plate spline gridlines and coloured meshes of negative shape scores of PC1. (B). Thin plate spline gridlines and coloured meshes of positive shape scores of PC1. (C). Thin plate spline gridlines and coloured meshes of negative shape scores of PC2. (D). Thin plate spline gridlines and coloured meshes of positive shape scores of PC2. Colour key expressed as centroid size percent.

skull roof (on the negative end) to a cranium with an elongated snout narrowed at the maxilla, posteriorly displaced orbits that open more dorsally, large pterygoid flanges and a sub-triangular skull roof. The block-2 PLS coefficients (Fig. 5A) of the five diet categories segregate the spiders and snails items to high negative values (ca −0.74 and −0.47 respectively), and only the vertebrates item shows high positive value (~0.45). The PLS1 scores show a high and significant correlation between blocks (Fig. 5A and Table 2; r = 0.723, $p < 0.0001$ after 10,000 rounds of permutation tests). While the juveniles lie on the double negative quadrant (with highly negatives values on block-2), the sub-adults lie near the zero values (but slightly displaced on negatives values of block-1) and the adults lie on the double positive quadrant.

Figs. 6 and 7 show the regression results of shape versus log-transformed centroid size for *C. latirostris* and *C. yacare*, respectively. Changes of colours observed in adults (Figs. 6C and 7C) could be interpreted as follow: gray means no relative changes and indicates isometry; red means relative increase in size and indicates positive allometry; blue means relative decrease in size and indicates negative allometry. Both regression models were significant after 10,000 permutation rounds (p-value < 0.0001). Allometric scaling explains 37.19% of shape variation in *C. latirostris* and 32.98% in *C. yacare*. The angular comparison between these two regression vectors (in their own shape space) was 65.407° (p-value < 0.0001; i.e., non-orthogonal). In addition, these two regression vectors are orthogonal to all the PCs except PC2. The angular comparison between these vectors (i.e., regressions and PC2) has a high vector angle of 66.83° for *C. latirostris* and an acute vector angle of 11.258º for *C. yacare* (both p-values < 0.0001). Similar angular values were obtained with the pooled within-group regression (66.088º and 10.575º respectively). Consequently, there is a common pattern of shape changes shared by the two caiman species during ontogeny and in the PC2 (see the similar colour patterns in Figs. 3C–D, 6B–C and 7B–C) that will be not described here (see PC2 shape changes above for a detailed description).

Angular comparisons between regression analyses and PLS of each

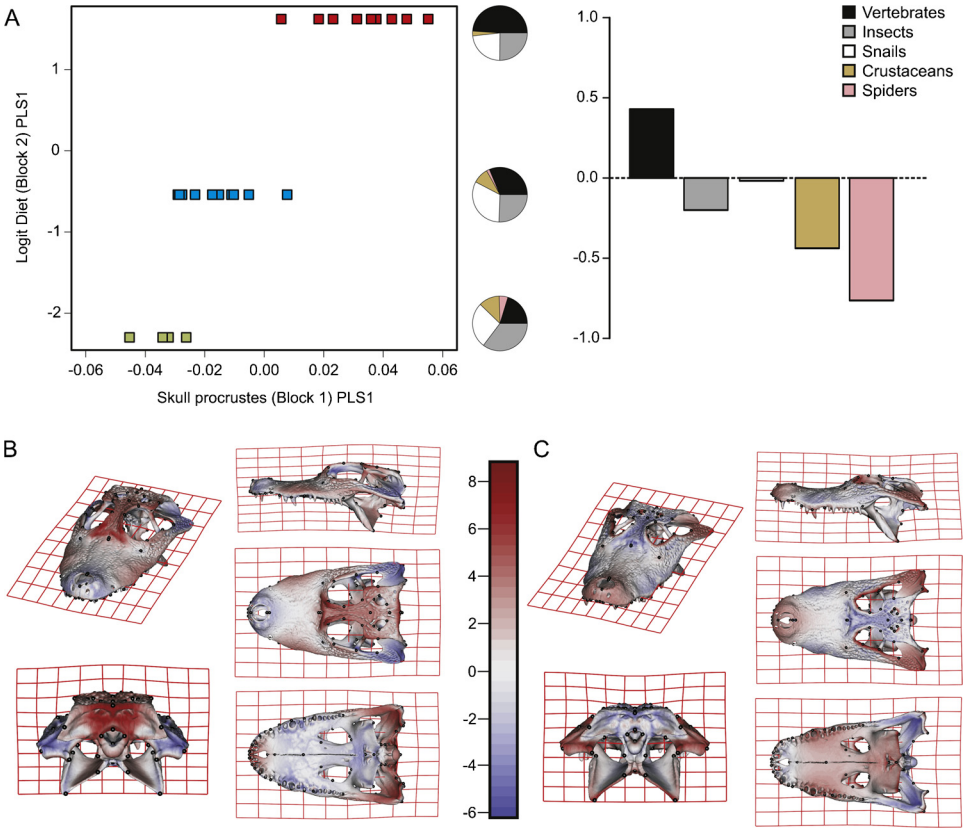

Fig. 4. Analysis of PLS of the Procrustes coordinates (Block1) and Logit diet (Block2) for *Caiman latirostris*. (A). Scores of first pair of PLS for juveniles (green squares), sub-adults (blue squares) and adults (red squares); pie charts depict dietary composition by age stage; and pairwise correlation coefficients between diet PLS axis and each dietary category (logit-transformed). (B). Thin plate spline gridlines and colored meshes of negative shape score. (C). Thin plate spline gridlines and colored meshes of positive shape score. Colour key expressed as centroid size per mille.

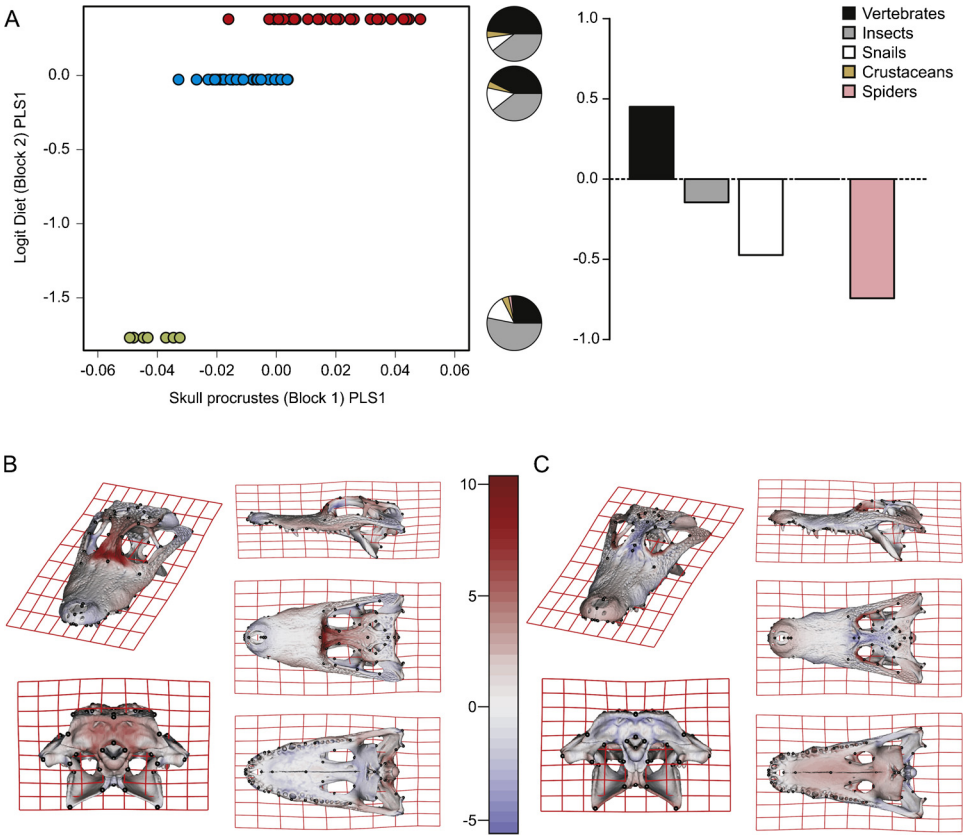

Fig. 5. Analysis of PLS of the Procrustes coordinates (Block1) and Logit diet (Block2) for *Caiman yacare*. (A). Scores of first pair of PLS for juveniles (green circles), sub-adults (blue circles) and adults (red circles); pie charts depict dietary composition by age stage; and pairwise correlation coefficients between diet PLS axis and each dietary category (logit-transformed). (B). Thin plate spline gridlines and colored meshes of negative shape score. (C). Thin plate spline gridlines and colored meshes of positive shape score. Colour key expressed as centroid size per mille.

Table 2
Partial Least Squares analyses for each species.

Species	Pair of axes	Singular value	S.v. *p*-value	% Total covar.	Correlation	Corr. *p*-value
Caiman yacare	PLS1	0.0105011	< 0.0001	92.72	0.72282	< 0.0001
	PLS2	0.00294259	0.0021	7.28	0.51045	0.1074*
Caiman latirostris	PLS1	0.04027853	< 0.0001	99.121	0.89588	0.0001
	PLS2	0.00379232	0.1945*	0.879	0.71512	0.1114*

PLS: Partial Least Squares; S.v. *p*-value: permutation test on Singular values; % Total covar.: Total covariance percent; Correlation: Pearson correlation coefficients between PLS scores of Block 1 and Block 2; Corr. *p*-value: permutation test on correlation values from the PLS scores.
All tests were significant at 0.05 level after 10000 round permutations, except those tagged by an asterisk.

species show that their vector of shape changes were more similar for *C. latirostris* than for *C. yacare* (angle between vectors of 11.87º; $p < 0.00001$ and 16.12º; $p < 0.00001$, respectively). Additionally, both are acute angles, showing a close relationship between distinctive traits on each species that varies during ontogeny which are related to changes in their feeding behavior (i.e., PLS results).

Fig. 8 illustrates the morphological differences between both species that change during ontogeny which have taxonomic implications. The nasals contact the naris only in juveniles of *C. yacare* (Fig. 8A) and are posteriorly displaced in the adults (Fig. 8C), while in *C. latirostris* they always contact the naris forming their posterior border (Fig. 8B and D). In the orbital region of young specimens of *C. yacare*, the frontal contacts the nasals (Fig. 8A) but they become progressively separated in the adults because the prefrontals interpose between them (Fig. 8C). In contrast, in *C. latirostris*, the frontal typically contacts the nasals (except in MLP-R.5364 and MLP-R.5809; Fig. 8B and D). At the temporal region, the supraoccipital is proportionately short in juveniles of *C. yacare* (Fig. 8A and C), while it keeps the same proportion in *C. latirostris* (Fig. 8B and D).

4. Discussion

4.1. Missing landmark estimation

Our study, contrary to Arbour and Brown (2014), showed that the mean and cumulative mean error per specimen relative to centroid size was lower in TPS reconstruction than in the REG, MS and BPCA methods (supporting information Data S1 in the supplementary online Appendix). It is worthwhile to note that unlike the examples of Arbour and Brown (2014), we digitized more landmarks than finally were used in this study, in order to improve missing landmark estimation. Moreover, we simulated the missing landmarks in the same way they were presented in our sample (see details in supporting information Data S1 in the supplementary online Appendix). Therefore, in spite of finding a general method for missing landmark estimation, we aimed to look for a stepwise procedure that would help us to solve our particular case. As a result, we used the TPS method based on the three most similar shapes within species (sensu Procrustes distances), to reconstruct those specimens with missing landmarks (see also Fernandez Blanco et al., 2014; Arnold et al., 2016; Handley et al., 2016; Mikula et al., 2016).

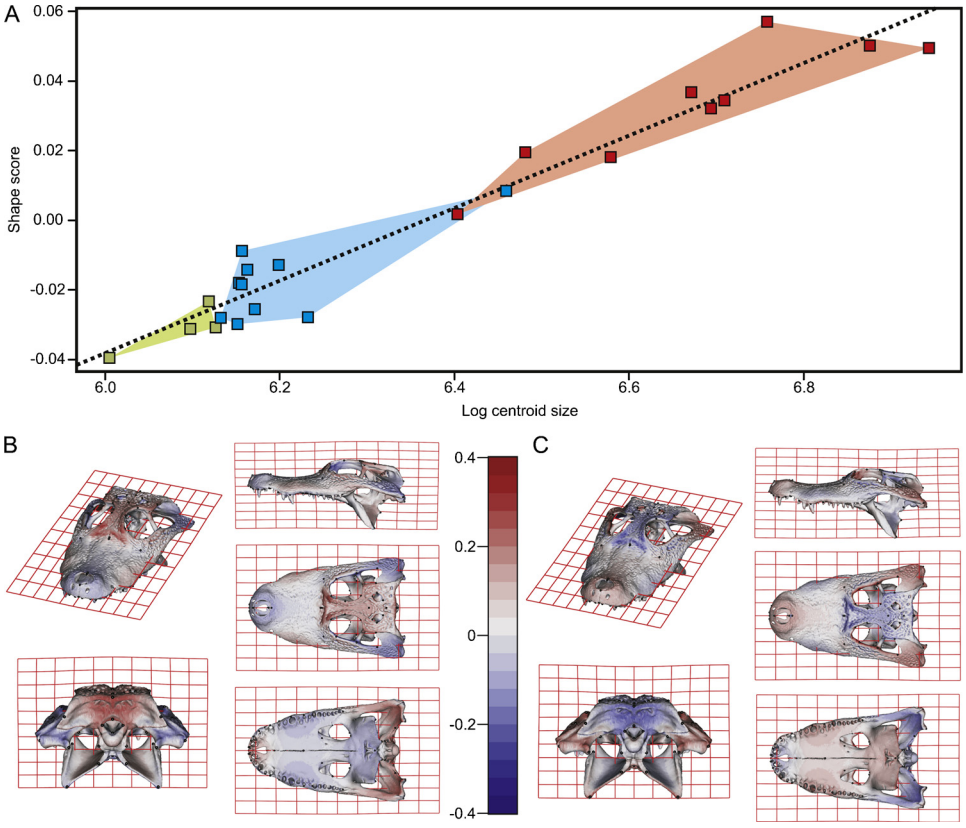

Fig. 6. Analysis of multivariate regression of the Procrustes coordinates against the log-transformed centroid size for *Caiman latirostris*. (A). Shape scores *vs* log CS. (B). Thin plate spline gridlines and coloured meshes of negative shape scores exaggerated three times. (C). Thin plate spline gridlines and coloured meshes of positive shape scores exaggerated three times. Colour key expressed as centroid size percent. Juveniles (green), sub-adults (blue), adults (red).

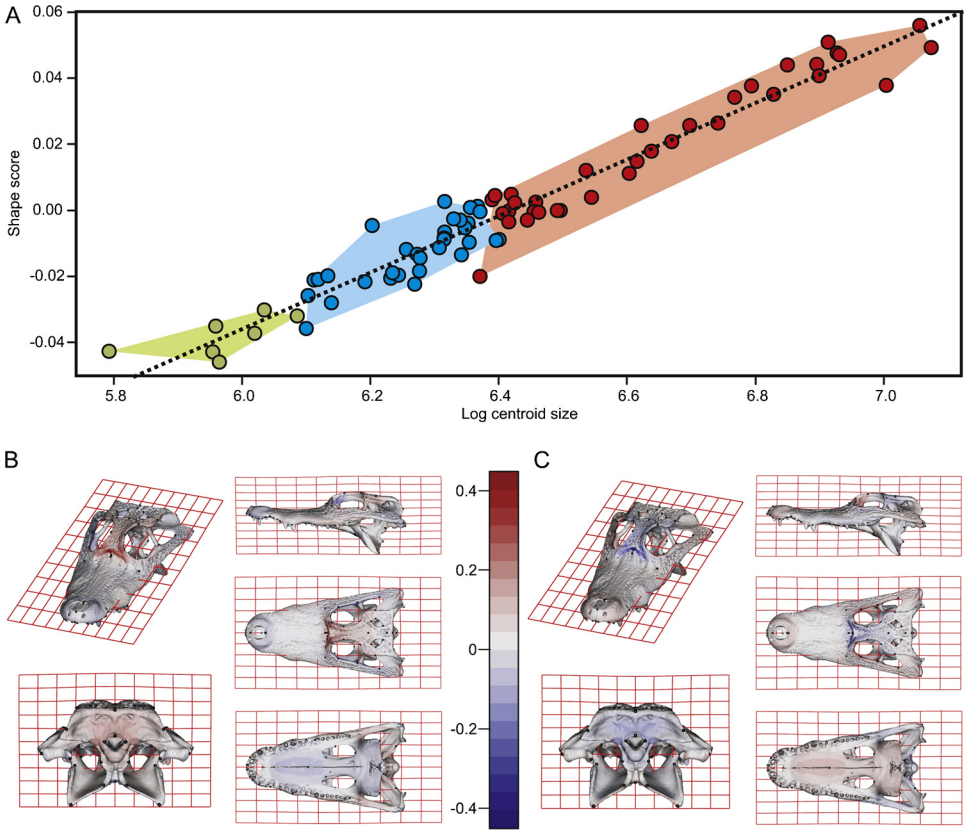

Fig. 7. Analysis of multivariate regression of the Procrustes coordinates against the log-transformed centroid size for *Caiman yacare*. (A). Shape scores vs log CS. (B). Thin plate spline gridlines and coloured meshes of negative shape scores exaggerated three times. (C). Thin plate spline gridlines and coloured meshes of positive shape scores exaggerated three times. Colour key expressed as centroid size percent. Juveniles (green), sub-adults (blue), adults (red).

4.2. Posthatching Ontogeny

Our results show that morphological changes found in this study have a meaningful significance related to both taxonomic and functional aspects. Both PCA and allometric analyses describe a mixture of taxonomic and functional aspects of shape, while the PLS shows an ecomorphological pattern. Although cranial morphology was found more related to taxonomy than ecology (Bogdanowicz et al., 2005; Cardini and Elton, 2008; Barčiová, 2009; Piras et al., 2011; Cassini, 2013; Foth et al., 2015; Murta-Fonseca and Fernandes, 2016), there are many examples of ecomorphological association even during ontogeny (e.g., Merino et al., 2005; Urošević et al., 2013; Segura et al., 2013, 2017; Segura, 2015; Olsen, 2017).

In the PCA, the cranial shape variation is more conspicuous between the two species of caiman than during ontogeny. Both species occupy different regions in the morphospace, mainly on PC1 (43.54% of total variance) which account for interspecific variation. This agrees with the findings of Watanabe and Slice (2014) on crocodylians, and also can be observed in some mammals (see Bastir et al., 2004; Segura et al., 2013 among others). However, the most common pattern when comparing close related species in tetrapods, is to find more shape variation during ontogeny than between species (see Witzmann et al., 2009 for *Temnospondyls*; Maiorino et al., 2013 for *Ticeratops*; Fuchs et al., 2015 for *Ursids*; Segura et al., 2017 for pantherines). In this study, the PC1 describes gracile (negative values) to robust (positive values) variation, and two very different morphologies across all postnatal (i.e., post-hatching) ontogenetic stages can be distinguish. *Caiman yacare* is the most gracile species and is characterized by a long, narrow and low cranium, while the most robust *C. latirostris* has a short, wide and high cranium. On the other hand, there are some previous studies that reveal that all extant jacarean species can be separated from each other based on their cranial shape (e.g., Fernandez Blanco et al., 2014; Foth et al., 2017).

Even though both caiman species have different skull shapes, they have similar growth patterns as their skulls undergo similar allometric shape changes (see also Fernandez Blanco et al., 2014; Foth et al., 2015, 2017). Comparable shape changes can be observed in PC2 (19.22%. of total variance) and in the regression vectors of *Caiman latirostris* and *C. yacare* (37.19% and 32.98% of shape variation explaining by allometric scaling) (see colour patterns in Figs. 3C–D, 6B–C and 7B–C). This common pattern registered with these last two analyses represents the transformation from juvenile to adult skull morphology, and it is supported by the increasing of the proportions of the snout (long, narrow and high) and pterygoid flanges, and by the decrease in sizes of the orbits (which also open more dorsally), temporal fenestrae, skull roof and foramen magnum. Although Watanabe and Slice (2014) did not study *C. latirostris* and *C. yacare*, they found the same changes in the orbits and temporal fenestrae in other species of crocodylians. This founding, according to the previous authors, constitutes a general morphological change in the cranial ontogeny of crocodylians. In the classic concept of allometry, a negatively allometric trait increases less in size than other traits or body size, while a positively allometric trait increases more in size relative to other traits or overall size (Mitteroecker et al., 2013). Alternatively, in geometric morphometrics all shape coordinates must be considered together in order to characterize the relative decrease (or increase) in size of specific parts accounted by the shape change vector (see colour patterns in Figs. 6B–C and 7B–C). Skulls of alligatorids imply the negative allometry of fenestrae (suborbital and infra and supra temporal) and neurocranium (orbits, skull roof, occipital plate, foramen magnum), and the positive allometry of splanchnocranium (rostrum, palate, pterigoids flanges) (see also Iordansky, 1973; Monteiro and Soares, 1997; Brochu, 2001; Fernandez Blanco et al., 2014, 2015; Watanabe and Slice 2014; Brown and Vavrek, 2015). Moreover, this general pattern (e.g., snout elongation and small orbits, among others) was also previously reported in temnospondyls (Witzmann et al., 2009), dinosaurs (Maiorino et al., 2013), and even it was recognized to be plesiomorphic to mammals with different methodologies (Emerson and Bramble, 1993; Cardini and

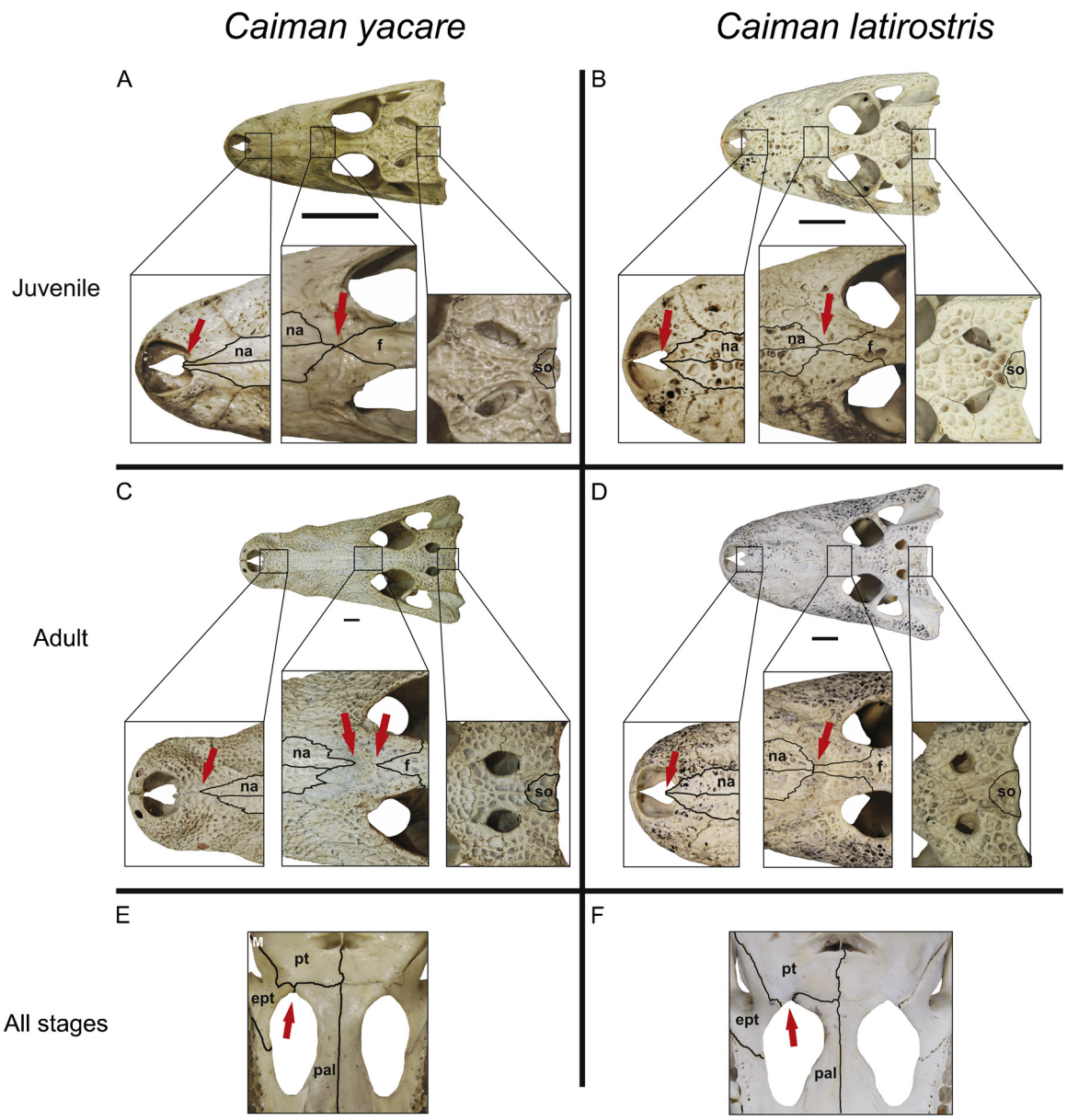

Fig. 8. Characters of systematic importance in (A, E) a juvenile specimen (MLP-R.5053) and (C) an adult specimen (MLP-R.43694) of *Caiman yacare*, and in (B, F) a juvenile specimen (MLP-R.5806) and (D) an adult specimen (MLP-R.6251) of *Caiman latirostris*. **Abbreviations: ept,** ectopterygoid; **fr**, frontal; **na**, nasal; **pal**, palatine; **pt**, pterygoid; **so**, supraoccipital. Scale bars equal 3 cm.

Polly, 2013; Flores et al., 2015). This leads us to propose that these allometric trends are the plesiomorphic condition, at least, for tetrapods.

Additionally to the common allometric shape change pattern of alligatorids, the caiman species analyzed in this study have shape changes that were found to be related to ontogenetic changes in the diet (food items). The correlation of cranial shape and diet is very high given the few discretized ontogenetic stages and explains 89.6% of the first PLS axes in *C. latirostris* (Fig. 4A and Table 2) and 72.3% in *C. yacare* (Fig. 5A; Table 2). In both species, axes of correlations are consistent with a juvenile cranial shape feeding mainly on invertebrates and an adult cranial shape feeding exclusively on vertebrates. Even though the size of the prey consumed increases throughout development as well as their frequency of consumption, predation on small prey never ceases (Santos et al., 1996; Melo, 2002; Borteiro et al., 2008). On the one hand, larger prey are stronger and exert more strength to escape. On the other hand, caimans require higher sideways bites in the crushing phase to reduce the prey to a suitable size for the ingestion. Consequently, this change in diet requires stronger skulls and larger adductor muscles. As individuals grow, the greater the prey size, the greater the musculature involved in the bite force. During ontogeny, caimans develop larger pterygoid flanges providing greater areas for the attachment of the *M. pterygoideus ventralis* and *dorsalis* (Holliday and Witmer, 2007; Holliday, 2009; Holliday et al., 2015; Sellers et al., 2017). These muscles are in charge of restricting movements to the sagittal plane during closure of the mouth to avoid dislocation of the mandible during feeding. Moreover, this shift is accompanied by other features such as a low occipital plate, a greater concavity of the posterior margin of the skull roof and a lateral expansion of the quadrate (with its condyle) and quadratojugal, that allow a greater development of the depressor mandibulae and the associated adductor muscles (*m. adductor mandibulae externus superficialis, m. adductor mandibulae externus medialis, m. adductor mandibulae externus profundus* and *m. adductor mandibulae posterior*; see Iordansky, 1964; Schumacher, 1973; Cleuren and De Vree, 2000; Holliday and Witmer, 2007; Bona and Desojo, 2011). This is also complemented with changes in the rostrum

(large premaxillae, high and robust snout) that result in a stronger skull. On the whole, all together these changes could be interpreted as an adaptation towards capturing and crushing larger prey sizes such as vertebrates (Dodson, 1975; Webb et al., 1978; Hutton, 1987).

Additionally, there are morphological differences between juveniles of both caiman species that could be related to the item food hardness. In the first pair of PLS, the juvenile shape of *C. latirostris* is related to a feeding based mainly on spiders and crustaceans (shrimps and crabs; Borteiro et al., 2008), whereas *C. yacare* juvenile shape relays on spiders and snails (Santos et al., 1996). The shell of both fresh water crabs (*Trichodactylus*) and apple snails (*Pomacea*) consumed by each species of caiman (*C. latirostris* and *C. yacare*, respectively) differs on the stiffness of the material and the ability to resist cracking. There is no data available on mechanical properties of both prey species of caiman in the literature. However, there are few mechanical studies made on chitins of different invertebrates that support our statement (see Hepburn et al., 1975; Robalino and Mera, 2014; Gadgey and Bahekar, 2017 and references there in). Consequently, dissimilarities based mainly on skull proportions and position of naris, orbits and skull roof resume the two very different cranial morphologies (gracile and robust) and seem to be related to different aforementioned mechanical requirements. In addition, preferences and the use of habitat are different between species, a condition that is accentuated when both species coexist (Larriera and Imhof, 2006). While *C. latirostris* prefers lentic, shallow and vegetated environments (Medem, 1983; Yanosky, 1990; Larriera and Imhof, 2006; Poletta, 2011), *C. yacare* shows greater preferences for lotic and deeper water courses without much vegetation (Larriera and Imhof, 2006). Consequently, interspecific differences could be clarified in this way as it has been cited for other species of crocodylians (Magnusson et al., 1987). The elongated, narrow and flat structure of the skulls (specially the snout) of *C. yacare* would facilitate aquatic movements: long and narrow snout offers less resistance to water (Cleuren and De Vree, 2000). On the other hand, robust skulls (short and wide) of *C. latirostris* would be more suitable for movements and searching of food in shallow environments with greater vegetation (Borteiro et al., 2008). Supporting this idea, Magnusson et al. (1987) proposed that, in general terms, the variety of cranial shapes in crocodylians would be related to habitat. In this way, species with low and wide heads inhabit marshy areas, and species with long and thin snouts will develop in riparian habitats. The idea that the morphology of *C. latirostris* is associated with its more coastal habitats is also supported by the different sizes of the interorbital ridge in the two species. *C. latirostris* has more prominent interorbital ridges than *C. yacare*. Mertens (1943) suggests that the interorbital ridge of caimans serves to keep away mud and water plants from eyes as it lies slightly above the water surface when they float (Iordansky, 1973). Nevertheless, the analysis to what extent habitat selection influences the efficiency of foraging strategies is a field worth researching.

4.3. Morphological characters of systematic importance

Some cranial regions that change morphologically during ontogeny are linked to discrete morphological characters used in phylogenetic analyses. Many of these characters are recovered as autapomorphies/synapomorphies of different caimanine taxa (Norell, 1988; Brochu, 1999, 2004, 2010, 2011; Bona, 2007; Hastings et al., 2013, 2016; Fortier et al., 2014; Salas-Gismondi et al., 2015; Cidade et al., 2017). The antorbital region (including the snout) was specially sampled in this study to see if those characters vary ontogenetically. As a result, it could be corroborated that some features are modified significantly during ontogeny in the caiman species analyzed here. The contact of nasals with naris (character 82 from Salas-Gismondi et al., 2015; modified from Brochu, 1999, 2011; adapted from Norell, 1988 and Clark, 1994) varies in *Caiman yacare*, since they lose contact during growth (Fig. 8A and C), while nasals and naris are always in contact in *C. latirostris* (Fig. 8B and D). In the same way, the contact of prefrontals in the midline is a character used in systematics of Alligatoroidea and is recovered as a synapomorphy of *C. yacare* + *C. crocodilus* (Norell, 1988), as an apomorphy of *C. yacare* (Brochu, 1999), and even as a synapomorphy of the clade of caimanine that excludes *Gnatusuchus* and *Culebrasuchus* (Cidade et al., 2017). This character presents ontogenetic variation in *Caiman yacare*, in which prefrontals approach medially during growth until they contact in the midline in the late ontogeny (Fig. 8A and C). It should be noted that although in C. *latirostris* no ontogenetic variation was noticed (Fig. 8B and D), individual variation was detected for this character; in most of the specimens prefrontals do not contact each other but in two of them (a subadult and an adult individuals) the midline contact was observed. Concerning the supraoccipital exposure on dorsal skull roof, it shows ontogenetic (*C. yacare*) and interspecific variation (Fig. 8A and D) but it does not interfere the state of the character that applies for caimanines in systematics (e.g., Norell, 1988; Brochu, 1999, 2004, 2010, 2011; Bona, 2007; Hastings et al., 2013, 2016; Fortier et al., 2014; Salas-Gismondi et al., 2015).

Regarding the palate, the bones that border the suborbital fenestra (and the proportion in which one of them participate) do not vary during the ontogeny in *Caiman latirostris* and *C. yacare*. In *C. latirostris* the suborbital fenestra is bordered by palatines, ectopterygoids and pterygoids (broadly) (Fig. 8F), and in *C. yacare* it is bordered by palatines and ectopterygoids and, in some cases, by pterygoids minimally too (Fig. 8E). So, this feature does not vary ontogenetically but it does vary intraspecifically in *C. yacare*. Brochu (1999) describes that the posterior border of the suborbital fenestra in *C. yacare* is limited only by ectopterygoids and palatines. Moreover, some authors mention ontogenetic variation for this feature in alligatorids (e.g., *C. yacare*, Norell, 1988; *Alligator mississippiensis*, Brochu, 1999), and it is proposed by Norell (1988) as supporting clades (i.e., “pterygoids participates slightly in the formation of the posterior border of this fenestra”, unambiguous synapomorphy for Jacarea: *Caiman* + *Melanosuchus*; Norell, 1988). The participation of the pterygoid in the posterior margin of the suborbital fenestra was included in crocodylian phylogenetic analyses only by Norell (1988). More recent studies described and discussed this feature in morphological descriptions of caimanines (e.g., *C. crocodilus* and *Mourasuchus*; Brochu, 1999; Bona, 2007; Bona et al., 2012) but they did not include it anymore in the morphological matrix. On the whole, all the cranial variation detected in this study and mentioned above need to be kept in mind during phylogenetic matrix building, and those continuous and polymorphic characters should be scored as such (Watanabe, 2016).

5. Conclusions

The TPS method was the most suitable for estimating missing landmarks in our sample. The common morphological changes occurring during ontogeny respond partly to a general allometric pattern shared by different tetrapod lineages. In addition, they also reflect the same mechanical requirements for crushing and killing in both species which seem to be driven by ontogenetic changes in the diet from invertebrates to vertebrates. Interspecific differences respond to the two well differentiated cranial morphologies (gracile and robust) that reflect food item stiffness and toughness as well as different habitat preferences. However, more ecological and biomechanical studies are needed to corroborate these last hypotheses. Lastly, it has been demonstrated that some discrete morphological cranial characters present inter- and intraspecific variation in caiman species which must be used and incorporated carefully in future phylogenetic analyses of Crocodylia.

Acknowledgements

We would like to thank Sergio F. Vizcaíno for having kindly allowed us to use the Microscribe. We want to acknowledge Jorge D. Williams

(MLP), Leandro Alcalde (MLP) and Julián Faivovich (MACN) for giving us access to the herpetological collections, and to the people of the "Estancia El Cachapé" (Chaco province) who provided us new material to study (now in herpetological collections). We are very grateful to Alejandro Otero for helping us with some figures and to the reviewers for the constructive comments. Finally, we thank Julia B. Desojo for the logistics. This work is a contribution to the research projects of the National Agency for Scientific and Technological Promotion [PICT 2016 N° 0159, PICT 2015 Nº 2389 and PICT 2008 N° 0143], of the Council National Scientific and Technical Research [PIP 1054], of the National University of La Plata [N747] and of National University of Luján [CDD-CB 650/14].

Appendix A. Supplementary data

Supplementary material related to this article can be found, in the online version, at doi:https://doi.org/10.1016/j.zool.2018.06.003.

References

Arbour, J.H., Brown, C.M., 2014. Incomplete specimens in geometric morphometric analyses. Methods. Ecol. Evol. 5, 16–26.
Arnold, P., Forterre, F., Lang, J., Fischer, M.S., 2016. Morphological disparity, conservatism, and integration in the canine lower cervical spine: insights into mammalian neck function and regionalization. Mamm. Biol. 81, 153–162.
Ayarzagüeña, J., 1983. Ecología del caiman de anteojos o baba (*Caiman crocodilus* L.) en los llanos de Apure (Venezuela). Doñana 10, 1–136.
Barčiová, L., 2009. Advances in insectivore and rodent systematics due to geometric morphometrics. Mammal Rev. 39, 80–91.
Bastir, M., Rosas, A., Kuroe, K., 2004. Petrosal orientation and mandibular ramus breadth: evidence for an integrated petroso-mandibular developmental unit. Am. J. Phys. Anthropol. 123, 340–350.
Benton, M.J., Clark, J.M., 1988. Archosaur phylogeny and the relationships of the Crocodylia. In: Benton, M.J. (Ed.), The Phylogeny and Classification of the Tetrapods, volume 1: Amphibians, Reptiles, Birds. Systematics Association Special Volume 35App. Clarendon Press, Oxford, pp. 295–338.
Bogdanowicz, W., Juste, J., Owen, R.D., Sztencel, A., 2005. Geometric morphometrics and cladistics: testing evolutionary relationships in mega-and microbats. Acta Chiropterol. 7, 39–49.
Bona, P., 2007. Una nueva especie de *Eocaiman* Simpson (Crocodylia, Alligatoridae) del Paleoceno Inferior de Patagonia. Ameghiniana 44, 435–445.
Bona, P., Degrange, F.J., Fernández, M.S., 2012. Skull anatomy of the bizarre crocodylian *Mourasuchus nativus* (Alligatoridae, Caimaninae). Anat. Record 296, 227–239.
Bona, P., Desojo, J.B., 2011. Osteology and cranial musculature of *Caiman latirostris* (Crocodylia: Alligatoridae). J. Morphol. 272, 1–16.
Bona, P., Fernandez Blanco, M.V., Scheyer, T.M., Foth, C., 2017. Shedding light on the taxonomic diversity of the South American Miocene caimans: the status of *Melanosuchus fisheri* Medina, 1976 (Crocodylia, alligatoroidea). Ameghiniana 54, 681–687.
Bookstein, F.L., 1991. Morphometric Tools for Landmark Data: Geometry and Biology. Cambridge University Press, New York.
Borteiro, C., Gutiérrez, F., Tedrosa, M., Kolenc, F., 2008. Food habits of the broad-snouted *Caiman* (*Caiman latirostris*: Crocodylia, Alligatoridae) in northwestern Uruguay. Studies Neotrop. Fauna Environ. 1, 1–6.
Brochu, C.A., 1999. Phylogenetics, taxonomy and historical biogeography of Alligatoroidea. J. Vertebr. Paleontol. 6, 9–100.
Brochu, C.A., 2001. Crocodylian snouts in space and time: phylogenetic approaches toward adaptive radiation. Amer. Zool. 41, 564–585.
Brochu, C.A., 2004. Alligatorine phylogeny and the status of *Allognathosuchus* Mook, 1921. J. Vertebr. Paleontol. 14, 857–873.
Brochu, C.A., 2010. A new alligatorid from the lower Eocene Green River Formation of Wyoming and the origin of caimans. J. Vertebr. Paleontol. 30, 1109–1126.
Brochu, C.A., 2011. Phylogenetic relationships of *Necrosuchus ionensis* Simpson, 1937 and the early history of caimanines. Zool. J. Linn. Soc. 163, S228–S256.
Brown, C.M., Vavrek, M.J., 2015. Small sample sizes in the study of ontogenetic allometry; implications for palaeobiology. PeerJ 3, e818.
Busack, S.D., Pandya, S., 2001. Geographic variation in *Caiman crocodilus* and *Caiman yacare* (Crocodylia: Alligatoridae): systematic and legal implications. Herpetologica 57, 294–312.
Cardini, A., Elton, S., 2008. Variation in guenon skulls (I): species divergence, ecological and genetic differences. J. Hum. Evol. 54, 615–637.
Cardini, A., Polly, P.D., 2013. Larger mammals have longer faces because of size-related constraints on skull form. Nat. Commun. 4, 2458.
Carvalho, A.L., 1951. Os jacarés do Brasil. Arq. Mus. Nac. 42, 127–152.
Cassini, G.H., 2013. Skull geometric morphometrics and paleoecology of Santacrucian (late early Miocene; Patagonia) native ungulates (Astrapotheria, Litopterna, and Notoungulata). Ameghiniana 50, 193–216.
Cassini, G.H., Muñoz, N.A., Vizcaino, S.F., 2017. Morphological integration of native south american ungulate mandibles. A tribute to D'Arcy Thompson in the centennial of "on growth and form". PE-APA 17, 58–74.
Cassini, G.H., Vizcaíno, S.F., 2012. An approach to the biomechanics of the masticatory apparatus of Early Miocene (Santacrucian Age) South American Ungulates (Astrapotheria, Litopterna, and Notoungulata): moment arm estimation based on 3D landmarks. J. Mamm. Evol. 19, 9–25.
Cidade, G.M., Solórzano, A., Rincón, A.D., Riff, D., Hsiou, A.S., 2017. A new *Mourasuchus* (Alligatoroidea, Caimaninae) from the late Miocene of Venezuela, the phylogeny of Caimaninae and considerations on the feeding habits of *Mourasuchus*. PeerJ 5, e3056.
Clark, J.M., 1994. Patterns of evolution in Mesozoic Crocodyliformes. In: Fraser, N.C., Sues, H.D. (Eds.), The Shadow of the Dinosaurs: Early Mesozoic Tetrapods. Cambridge University Press, New York, pp. 84–97.
Cleuren, J., De Vree, F., 2000. Feeding in Crocodylians. In: Schwenk, K. (Ed.), Feeding. Academic Press, San Diego, pp. 337–358.
Daudin, F.M., 1802. Histoire Naturelle des Reptiles. Dufart F, Paris.
Dodson, P., 1975. Functional and ecological significance of relative growth in Alligator. J. Zool. 175, 315–355.
Drake, A.G., Klingenberg, C.P., 2008. The pace of morphological change: historical transformation of skull shape in St Bernard dogs. Proc. R. Soc. Lond. B: Biological Sciences 275, 71–76.
Dryden, I.L., Mardia, K.V., 1998. Statistical Shape Analysis. John Wiley & Sons, Chichester.
Emerson, S.B., Bramble, D.M., 1993. Scaling, allometry, and skull design. In: Hanken, J., Hall, B.K. (Eds.), The Skull. Volume 3: Functional and Evolutionary Mechanisms. Chicago University Press, Chicago, pp. 384–421.
Fernandez Blanco, M.V., Bona, P., Olivares, A.I., Desojo, J.B., 2015. Ontogenetic variation in the skulls of *Caiman*: the case of *Caiman latirostris* and *Caiman yacare* (Alligatoridae, Caimaninae). Herpetol. J. 25, 65–73.
Fernandez Blanco, M.V., Cassini, G.H., Bona, P., 2014. Variación morfológica craneana en *Caiman* (Alligatoridae, Caimaninae): estudio morfogeométrico de la ontogenia de las especies *Caiman latirostris* y *Caiman* yacare. Cs. Morfol. 16, 16–30.
Flores, D., Abdala, F., Martin, G., Giannini, N., Martinez, J., 2015. Post-weaning cranial growth in shrew opossums (Caenolestidae): A comparison with bandicoots (Peramelidae) and carnivorous marsupials. J. Mamm. Evol. 22, 285–303.
Fortier, D.C., Souza-Filho, J.P., Guilherme, E., Maciente, A.A.R., Schultz, C.L., 2014. A new specimen of *Caiman brevirostris* (Crocodylia, Alligatoridae) from the Late Miocene of Brazil. J. Vertebr. Paleontol. 34, 820–834.
Foth, C., Bona, P., Desojo, J.B., 2015. Intraspecific variation in the skull morphology of the black *Caiman Melanosuchus niger* (Alligatoridae, Caimaninae). Acta Zool. (Stockholm) 96, 1–13.
Foth, C., Fernandez Blanco, M.V., Bona, P., Torsten, M.S., 2017. Cranial shape variation in jacarean caimanines (Crocodylia, Alligatoroidea) and its implications in the taxonomic status of extinct species: the case of Melanosuchus fisheri. J. Morphol. 279, 259–273.
Fox, J., Weisberg, S., 2011. An {R} Companion to Applied Regression. URL:. 2nd ed. Sage, Thousand Oaks. http://socserv.socsci.mcmaster.ca/jfox/Books/Companion.
Fuchs, M., Geiger, M., Stange, M., Sánchez-Villagra, M.R., 2015. Growth trajectories in the cave bear and its extant relatives: an examination of ontogenetic patterns in phylogeny. BMC Evol. Biol. 15, 239.
Gadgey, K.K., Bahekar, A., 2017. Studies on extraction methods of chitin from crab shell and investigation of its mechanical properties. Int. J. Mech. Eng. Technol. 8, 220–231.
Goodall, C., 1991. Procrustes methods in the statistical analysis of shape. J. R. Stat. Soc. B. 53, 285–339.
Handley, W.D., Chinsamy, A., Yates, A.M., Worthy, T.H., 2016. Sexual dimorphism in the late Miocene mihirung *Dromornis stirtoni* (Aves: Dromornithidae) from the Alcoota Local Fauna of central Australia. J. Vertebr. Paleontol. 36, e1180298.
Hastings, A.K., Bloch, J.I., Jaramillo, C.A., Rincon, A.F., MacFadden, B.J., 2013. Systematics and biogeography of crocodylians from the Miocene of Panama. J. Vertebr. Paleontol. 33, 239–263.
Hastings, A.K., Reisser, M., Scheyer, T.M., 2016. Character evolution and the origin of Caimaninae (Crocodylia) in the New World Tropics: new evidence from the Miocene of Panama and Venezuela. J. Paleontol. 90, 317–332.
Hepburn, H.R., Joffe, I., Green, N., Nelson, K.J., 1975. Mechanical properties of a crab shell. Comp. Biochem. Physiol. 50, 551–554.
Holliday, C.M., 2009. New insights into dinosaur jaw muscle anatomy. Anat. Record 292, 1246–1265.
Holliday, C.M., Sellers, K.C., Vickaryous, M.K., Ross, C.F., Porro, L.B., Witmer, L.M., Davis, J.L., 2015. The functional and evolutionary significance of the crocodyliform pterygomandibular joint. Integr. Comp. Biol. 55, e81.
Holliday, C.M., Witmer, L.M., 2007. Archosaur adductor chamber evolution: integration of musculoskeletal and topological criteria in jaw muscle homology. J. Morphol. 268, 457–484.
Hrbek, T., Vasconcelos, W.R., Rebelo, G., Farias, I.P., 2008. Phylogenetic relationships of South American alligatorids and the caiman of Madeira River. J. Exp. Zool. A. 309, 588–599.
Hutton, J.M., 1987. Growth and feeding ecology of the Nile crocodile *Crocodylus niloticus* at Ngezi, Zimbabwe. J. Anim. Ecol. 56, 25–38.
Iordansky, N.N., 1964. The jaw muscles of the crocodiles and some relating structures of the crocodilian skull. Anat. Anz. 115, 256–280.
Iordansky, N.N., 1973. The Skull of the Crocodilia. Biology of the Reptilia 4, 201–262.
Klingenberg, C.P., 2011. MorphoJ: An integrated software package for geometric morphometrics. Molec. Ecol. Res. 11, 353–357.
Klingenberg, C.P., 2013. Cranial integration and modularity: insights into evolution and development from morphometric data. Hystrix 24, 43–58.
Klingenberg, C.P., Marugán-Lobón, J., 2013. Evolutionary covariation in geometric morphometric data: analyzing integration, modularity, and allometry in a phylogenetic context. Syst. Biol. 62, 591–610.

Larriera, A., Imhof, A., 2006. Proyecto yacaré. Cosecha de huevos para cría en granjas del género *Caiman* en la Argentina. In: Bolkovic, M.L., Ramadori, D. (Eds.), Manejo de Fauna Silvestre en la Argentina. Programas de Uso Sustentable. Dirección de Fauna Silvestre. Secretaría de Ambiente y Desarrollo Sustentable, Buenos Aires, pp. 51–64.
Linnaeus, C., 1758. Systema Naturae per Regna Trio Naturae, Secundum Classes, Ordines, Genera, Species, Cum Characteribus, Differentiis, Synonymis. Locis. Laurentii Salvii, Estocolmo.
Magnusson, W.E., Da Silva, E.V., Lima, A.P., 1987. Diets of Amazonian Crocodilians. J. Herpetol. 21, 85–95.
Maiorino, L., Farke, A.A., Kotsakis, T., Piras, P., 2013. Is *Torosaurus Triceratops*? Geometric morphometric evidence of late maastrichtian ceratopsid dinosaurs. PLoS One 8, e81608.
Medem, F., 1983. Los Crocodylia de Sur América. Carrera, Bogotá.
Melo, M.T.Q., 2002. Dieta do *Caiman latirostris* no Sul do Brasil. In: Verdade, L.M., Larriera, A. (Eds.), La conservación y el Manejo de Caimanes y Cocodrilos de América Latina. CN Editoria, Piracicaba, São Paulo, pp. 119–125.
Merino, M.L., Milne, N., Vizcaíno, S.F., 2005. A cranial morphometric study of deer (Mammalia, Cervidae) from Argentina using three-dimensional landmarks. Acta Theriol. 50, 91–108.
Mertens, R., 1943. Die rezenten Krokodile des Natur-Museums Senckenberg. Sencken 26, 252–312.
Mikula, O., Radim, Š., Aghová, T., Mbau, J.S., Katakweba, A.S., Sabuni, C.A., Bryja, J., 2016. Evolutionary history and species diversity of African pouched mice (Rodentia: Nesomyidae: *Saccostomus*). Zool. Scr. 45, 595–617.
Mitteroecker, P., Bookstein, F., 2008. The evolutionary role of modularity and integration in the hominoid cranium. Evolution 62, 943–958.
Mitteroecker, P., Gunz, P., Bernhard, M., Schaefer, K., Bookstein, F.L., 2004. Comparison of cranial ontogenetic trajectories among great apes and humans. J. Hum. Evol. 46, 679–698.
Mitteroecker, P., Gunz, P., Windhager, S., Schaefer, K., 2013. A brief review of shape, form, and allometry in geometric morphometrics, with applications to human facial morphology. Hystrix 24, 59–66.
Monteiro, L.R., Cavalcanti, M.J., Sommer III, H.J.S., 1997. Comparative ontogenetic shape changes in the skull of *Caiman* species (Crocodylia, Alligatoridae). J. Morphol. 231, 53–62.
Monteiro, L.R., Soares, M.A., 1997. Allometric analysis of the ontogenetic variation and evolution of the skull in *Caiman* Spix, 1825 (Crocodylia, Alligatoridae). Herpetologica 53, 62–69.
Muñoz, N.A., Cassini, G.H., Candela, A.M., Vizcaíno, S.F., 2017. Ulnar articular surface 3-D landmarks and ecomorphology of small mammals: A case of study in two Early Miocene typotheres (Notoungulata) from Patagonia. Earth Env. Sci. T. R. So. 106, 315–323.
Murta-Fonseca, R.A., Fernandes, D.S., 2016. The skull of *Hydrodynastes gigas* (Duméril, Bibron & Duméril, 1854) (Serpentes: Dipsadidae) as a model of snake ontogenetic allometry inferred by geometric morphometrics. Zoomorphology 135, 233–241.
Norell, M.A., 1988. Cladistic approaches to paleobiology as applied to the phylogeny of alligatorids. PhD Thesis. Yale University, New Haven p. 272, Inédita.
Oaks, J.R., 2011. A time-calibrated species tree of Crocodylia reveals a recent radiation of the true crocodiles. Evolution 65, 3285–3297.
Olsen, A.M., 2017. Feeding ecology is the primary driver of beak shape diversification in waterfowl. Funct. Ecol. 31, 1985–1995.
Pinheiro, A.E.P., Fortier, D.C., Pol, D., Campos, D.A., Bergqvist, L.P., 2013. A new *Eocaiman* (Alligatoridae, Crocodylia) from the Itaboraí Basin, Paleogene of Rio de Janeiro. Brazil. Hist. Biol. 25, 327–337.
Piras, P., Salvi, D., Ferrara, G., Maiorino, L., Delfino, M., Pedde, L., Kotsakis, T., 2011. The role of post-natal ontogeny in the evolution of phenotypic diversity in *Podarcis* lizards. J. Evolution. Biol. 24, 2705–2720.
Poletta, G.L., 2011. Monitoreo de daño inducido por plaguicidas en *Caiman latirostris* (Yacaré overo) como organismo centinela de los humedales de Argentina. Doctoral Disertation. Facultad de Ciencias Exactas y Naturales. Universidad de Buenos Aires p. 229.
R Development Core Team, 2017. R: A language and environment for statistical computing, software. R Foundation for Statistical Computing, Vienna. https://www.R-project.org/.
Robalino, J.D., Mera, J.E.Y., 2014. Influencia del alimento balanceado con tres niveles de inclusión de harina de cáscara de huevo, en el crecimiento y en la resistencia a la fractura de la concha del "churo", *Pomacea maculata* (Ampullaridae), cultivados en jaulas, en el centro de investigación, experimentación y enseñanza, piscigranja quistococha. PhD Thesis. Universidad Nacional De La Amazonia Peruana, Iquitos p. 55, Inédita.
Rohlf, F.J., 1999. Shape statistics: Procrustes superimpositions and tangent spaces. J Classif. 16, 197–223.
Rohlf, F.J., Corti, M., 2000. Use of two-block partial least-squares to study covariation in shape. Syst. Biol. 49, 740–753.
Salas-Gismondi, R., Flynn, J.J., Baby, P., Tejada-Lara, J.V., Claude, J., Antoine, P.-O., 2016. A new 13 million year old Gavialoid Crocodylian from Proto-Amazonian mega-wetlands reveals parallel evolutionary trends in skull shape linked to longirostry. PLoS One 11, e0152453.
Salas-Gismondi, R., Flynn, J.J., Baby, P., Tejada-Lara, J.V., Wesselingh, F.P., Antoine, P.O., 2015. A Miocene hyperdiverse crocodylian community reveals peculiar trophic dynamics in proto-Amazonian mega-wetlands. P. R. Soc. London 282, 20142490.
Santos, S.A., Stoll, M., Silva, M., Campos, Z., Magnusson, W.E., Mourão, G., 1996. Diets of *Caiman crocodilus yacare* from different habitats in the Brazilian Pantanal. Herpetol J. 6, 111–117.
Schlager, S., 2017. Morpho and Rvcg-Shape Analysis in R. In: Zheng, G., Li, S., Szekely, G. (Eds.), Statistical Shape and Deformation Analysis. Academic Press, Cambridge, pp. 217–256.
Schumacher, G.H., 1973. The head muscles and hyolaryngeal skeleton of turtles and crocodilians. Biology of the Reptilia 4, 101–200.
Segura, V., 2015. A three-dimensional skull ontogeny in the bobcat (*Lynx rufus*) (Carnivora: Felidae): a comparison with other carnivores. Can. J. Zool. 93, 225–237.
Segura, V., Cassini, G.H., Prevosti, F.J., 2017. Three-dimensional cranial ontogeny in pantherines (*Panthera leo*, *P. onca*, *P. pardus*, *P. tigris*; Carnivora:, Felidae). Biol. J. Linn. Soc. 120, 210–227.
Segura, V., Prevosti, F.J., Cassini, G.H., 2013. Cranial ontogeny in the Puma lineage, *Puma concolor*, *Herpailurus yagouaroundi*, and *Acinonyx jubatus* (Carnivora: Felidae): a three-dimensional geometric morphometric approach. Zool. J. Linn. Soc. 169, 235–250.
Sellers, K.C., Middleton, K.M., Davis, J.L., Holliday, C.M., 2017. Ontogeny of bite force in a validated biomechanical model of the American alligator. J. Exp. Biol. 220, 2036–2046.
Simpson, G.G., 1937. An ancient eusuchian crocodile from Patagonia. Am. Mus. Novit. 965, 1–20.
Spix, J.B., 1825. Animalia Nova Sive Species Novae Lacertarum. Quas in Itinere per Brasiliam Annis MDCCCXVII–MDCCCXX Jussu et Auspiciis Maximiliani Josephi I. Bavariae Regis.
Urošević, A., Ljubisavljević, K., Ivanović, A., 2013. Patterns of cranial ontogeny in lacertid lizards: morphological and allometric disparity. J. Evolution. Biol. 26, 399–415.
Vanzolini, P.E., Gomes, N., 1979. Notes on the ecology and growth of Amazonian caimans (Crocodylia, Alligatoridae). Pap. Avul. Zool. 32, 205–216.
Verdade, L.M., 2000. Regression equations between body and head measurements in the broad-snouted caiman (*Caiman latirostris*). Rev. Bras. Biol. 60, 469–482.
Warton, D.I., Hui, F.K.C., 2011. The arcsine is asinine: the analysis of proportions in ecology. Ecology 92, 3–10.
Watanabe, A., 2016. The impact of poor sampling of polymorphism on cladistic analysis. Cladistics 32, 317–334.
Watanabe, A., Slice, D.E., 2014. The utility of cranial ontogeny for phylogenetic inference: a case study in crocodylians using geometric morphometrics. J. Evolution. Biol. 27, 1078–1092.
Webb, G.J.W., Manolis, S.C., Buckworth, R., 1982. *Crocodylus johnstoni* in the McKinlay River Area, NTI. Variation in the diet, and a new method of assessing the relative importance of prey. Aust. J. Zool. 30, 877–899.
Webb, G.J.W., Messel, H., Crawford, J., Yerbury, M.J., 1978. Growth rate of *Crocodylus porusus* (Reptilia: Crocodilia) from Arnhem Land, Northern Australia. Aust. Wildlife Res. 5, 385–399.
Witzmann, F., Scholz, H., Ruta, M., 2009. Morphospace occupation of temnospondyl growth series: a geometric morphometric approach. Alcheringa 33, 237–255.
Wu, X.B., Xue, H., Wu, L.S., Zhu, J.L., Wang, R.P., 2006. Regression analysis between body and head measurements of Chinese alligators (*Alligator sinensis*) in the captive population. Anim. Biodiv. Conserv. 29, 65–71.
Yanosky, A.A., 1990. Histoire naturelle du Caiman à museau large (*Caiman latirostris*), un Alligatoriné mal connu (1). Rev. fr. Aquariol. Herpétol. 17, 19–31.